

# Impact of Electroforming Current on Self-Compliance Resistive Switching in an ITO/Gd:SiO<sub>x</sub>/TiN Structure

Hsueh-Chih Tseng, Ting-Chang Chang, *Senior Member, IEEE*, Yi-Chun Wu, Sei-Wei Wu, Jheng-Jie Huang, Yu-Ting Chen, Jyun-Bao Yang, Tzu-Ping Lin, Simon. M. Sze, *Life Fellow, IEEE*, Ming-Jinn Tsai, Ying-Lang Wang, and Ann-Kuo Chu

**Abstract**—This letter investigates self-compliance behavior for nonvolatile resistance random access memory using the indium tin oxide (ITO)/Gd:SiO<sub>x</sub>/TiN structure. Different current compliances in the electroforming process results in different trends in the set process, including a different self-compliance scale and one- or two-step set behaviors. The oxygen ions generated during the electroforming and set process drift to ITO, inducing a semiconductor-like ITO interface formation, which can be regarded as a self-built series resistor.

**Index Terms**—Indium tin oxide (ITO), resistance switching, resistive random access memory (ReRAM), self-built current compliance.

## I. INTRODUCTION

RECENTLY, portable electronics have attracted worldwide attention. Hence, transistor, TFT display, and non-volatile memory have been broadly utilized due to its desirable properties [1]–[4]. Conventional nonvolatile memory suffers from certain physical limitations due to its continual scaling down, such as an insufficient tunneling oxide thickness [1]. Hence, resistive random access memory (ReRAM) has attracted considerable interest for use in the next generation of nonvolatile memory devices as an alternative solution [5]–[7]. In addition, the development of a current-compliance element, such as a transistor or diode has been regarded as an important issue to commercialize ReRAM. The use

Manuscript received March 20, 2013; revised April 8, 2013; accepted April 16, 2013. Date of publication May 15, 2013; date of current version June 24, 2013. This work was supported in part by National Science Council Core Facilities Laboratory for Nano-Science and Nano-Technology in Kaohsiung-Pingtung area, and in part by the National Science Council of the Republic of China under Contract NSC-100-2120-M-110-003. The review of this letter was arranged by Editor T. Wang.

H.-C. Tseng, Y.-C. Wu, J.-J. Huang, and T.-P. Lin are with the Department of Physics, National Sun Yat-Sen University, Kaohsiung 804, Taiwan (e-mail: tcchang@mail.phys.nsysu.edu.tw).

T.-C. Chang is with the Department of Physics, National Sun Yat-Sen University, Kaohsiung 804, Taiwan and also with the Advanced Optoelectronics Technology Center, National Cheng Kung University, Tainan 70101, Taiwan.

S.-W. Wu and S. M. Sze are with the Department of Electronics Engineering, National Chiao Tung University, Hsinchu 30050, Taiwan.

Y.-T. Chen, J.-B. Yang, and A.-K. Chu are with the Department of Photonics, National Sun Yat-Sen University, Kaohsiung 804, Taiwan.

M.-J. Tsai is with the Nanoelectronic Technology Division, Electronics and Optoelectronics Research Lab/ITRI, Hsinchu, 31040, Taiwan.

Y.-L. Wang is with the Taiwan Semiconductor Manufacturing Company, Hsinchu 300-77, Taiwan.

Color versions of one or more of the figures in this letter are available online at <http://ieeexplore.ieee.org>.

Digital Object Identifier 10.1109/LED.2013.2259135

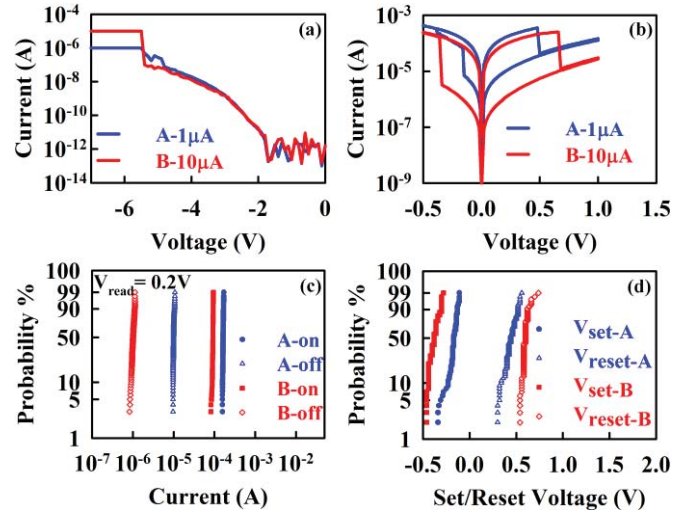


Fig. 1. (a) Electroforming process at 1 and 10  $\mu\text{A}$ . (b) Bipolar resistance switching for different current compliance processes. (c) Statistical data for ON/OFF ratio. (d) Statistical data of operation voltage, including set and reset voltages.

of gadolinium silicate (GdSiO) as a thermally-stable high-k gate dielectric has been investigated in a gate-first integration scheme [8]. Recently, doping metal within the SiO<sub>x</sub> as the ReRAM has been the focus of many studies [9], [10]. Up to now, however, the application of GdSiO in the resistive switching field has not been researched.

## II. EXPERIMENT

A Gd:SiO<sub>x</sub> thin film of about 10 nm was deposited on a TiN/Si substrate by reactive magnetron RF co-sputtering the SiO<sub>2</sub> and Gd targets in Ar (30 SCCM) ambience at room temperature. Then the indium tin oxide (ITO) top electrode (TE) was deposited and patterned by the lift-off process. The devices then underwent the electroforming process with a current compliance to activate. The different current-compliance of this electroforming process can form varied self-compliance properties. All electrical characteristics were measured with an Agilent B1500 semiconductor parameter analyzer. During these measurements, bias was applied to the TiN bottom electrode (BE) while the ITO TE was ground. This device exhibits a self-compliance property without an external current compliance element.

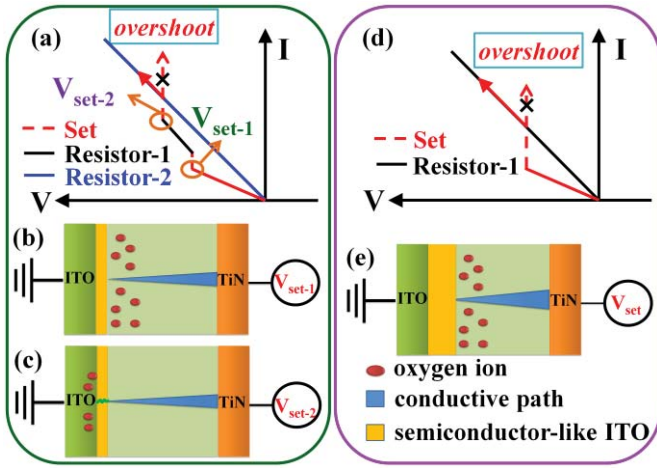


Fig. 2. Schematic diagrams of set process in (a)–(c) low-current compliance process, and (d)–(e) high-current compliance process.

### III. RESULT AND DISCUSSION

Fig. 1(a) shows different current compliances during the electroforming process, those of 1 and 10  $\mu\text{A}$ , which are necessary to activate the ReRAM device and produce traps (such as vacancies or metal precipitates) and oxygen ions. Generally, the vacancy-type defects dominate the conductivity of ITO [11]. Hence, because the generated oxygen ions drift to the ITO electrode and oxidize with ITO, the oxygen ions can partially combine with oxygen vacancies of ITO, resulting in a semiconductor-like ITO interface layer. Fig. 1(b) shows the  $I$ - $V$  curves of the device after the electroforming process, detailing the typical bipolar resistance switching behaviors with predetermined operation conditions, but without external current compliance during the set process. During the set process, a self-compliance phenomenon can be observed due to the formation of the semiconductor-like ITO interface layer, which acts as a series resistor connection. Hence, higher current compliance in the electroforming process can produce more oxygen ions and form a larger series resistor connection, inducing a lower self-compliance property in the ITO/Gd:SiO<sub>x</sub>/TiN device. Fig. 1(c) shows an obvious memory window after the device has undergone a dc sweeping mode for 100 cycles. The comparisons in Fig. 1(d) indicate that the device with a higher current compliance during the electroforming process induces a larger  $V_{\text{set}}$  and  $V_{\text{reset}}$  because there is a larger total resistance in the equivalent circuit.

Fig. 1(b) shows different trends during the set process, including different self-current compliance behaviors and either a two-step (1  $\mu\text{A}$ ) or a one-step (10  $\mu\text{A}$ ) set process, as shown in Fig. 2(a) and (d). A schematic diagram of this different behavior is shown in Fig. 2. Fewer oxygen ions can be produced during the lower current-compliance electroforming process, resulting in the formation of a thinner semiconductor-like ITO interface. Therefore, as the applied bias increases at a critical voltage during the typical bipolar resistance switching set process, the oxygen ions can be created along with the conductive path formation. The oxygen ions next drift to and oxidize with ITO, as shown in Fig. 2(b). Subsequently, when the applied bias continues to increase, the ITO interface can

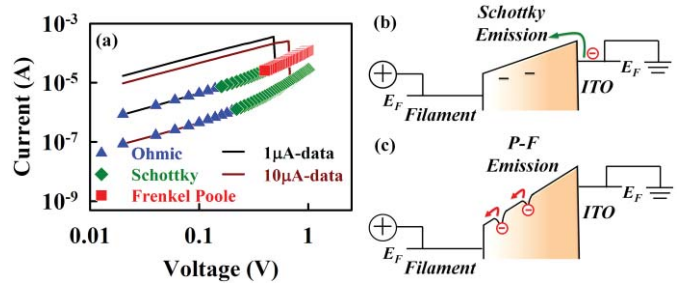


Fig. 3. (a) Current fitting result of resistance switching for low-current compliance process and high-current compliance process. Schematic energy band diagram of 1- $\mu\text{A}$  current compliance electroforming device in different bias regions, (b) Schottky emission, and (c) Frenkel–Poole emission.

undergo soft breakdown and cause another hetero-conductive-path, which acts as a self-built resistor [12], [13], as shown in Fig. 2(c). Accordingly, a higher current-compliance electroforming process can generate more oxygen ions and construct a better self-built resistor. Hence, this stronger ITO interface can tolerate the same bias stress without a second soft breakdown, as shown in Fig. 2(d) and (e). Consequently, the self-built resistor can prevent the device from overshooting and effectively reduce the operation current.

Fig. 3(a) shows the current fitting result of Fig. 1(b) for the metal/semiconductor current transportation mechanisms of Ohmic conduction, Schottky emission, and Frenkel–Poole emission. First, the conduction mechanism of LRS for both high-current compliance and low-current compliance electroforming processes follows Ohmic law due to the conductive path formation. Many studies have indicated that the different current compliance of electroforming process can lead to a varied amount of oxygen ions formation [14]. The low-current compliance of electroforming process cannot produce enough oxygen ions to oxidize the ITO [ITO + O<sub>2</sub> (poor)]. Fig. 2(a) has indicated that the oxidized ITO interface can be soft breakdown and creates another conductive path. The local Joule heating effect may cause the conductive path neighboring the ITO electrode to be transformed into discontinuous vacancies or defects after the reset process. Therefore, electrons must overcome the ITO/ITO + O<sub>2</sub> (poor) barrier in the low bias region, as shown in Fig. 3(b). Subsequently, when the applied bias increases, the vacancies or defects can provide another transport possibility and inducing a Frenkel–Poole emission dominated conductive mechanism, as shown in Fig. 3(c).

However, the formation of ITO + O<sub>2</sub> (rich) layer can be attributed to more oxygen ion generation and migration due to high-current compliance of electroforming process. This causes ITO interface to be better oxidized than that with low-current compliance treatment. Hence, in order to execute the reset process and achieve HRS, a larger reset voltage is necessary to cause a serious Joule heating effect. Then a more complete thermal oxidation can be triggered to break the conductive path resulting in a trapless ITO interface. Since electrons must overcome the ITO/ITO + O<sub>2</sub> (rich) barrier while undergoing a bias sweeping, Schottky emission can dominate the conductive mechanism. The comparison of high- and low-compliance electroforming processes in Fig. 3(a)

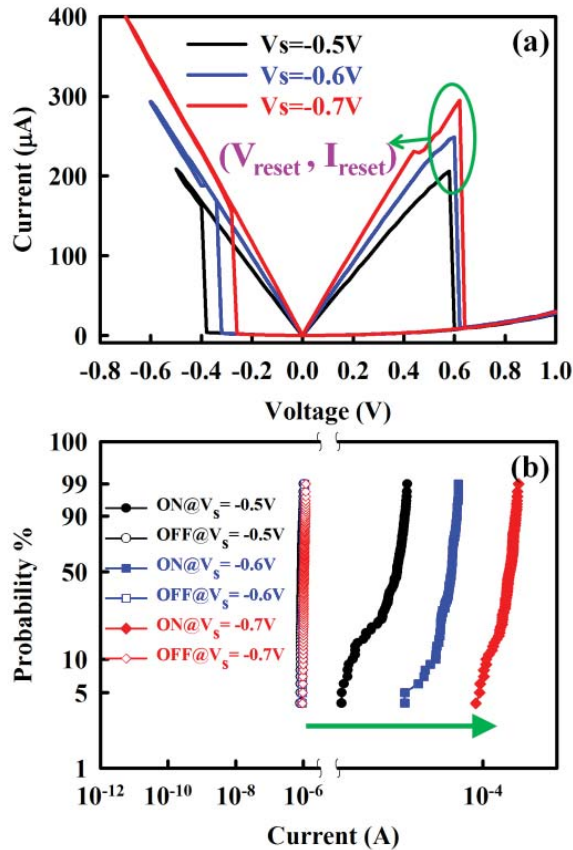


Fig. 4. (a) Different applied bias inducing multi-LRS. (b) Statistical data for multi-LRS while undergoing 100 cycling operations.

shows that only Schottky emission dominates the transport mechanism of HRS for high-compliance, unlike that for low-compliance.

Because the ITO/Gd:SiO<sub>x</sub>/Pt device exhibits a self-built current compliance function, different applied biases correspond to different resistances, similar to different current compliances inducing multi-LRS. Therefore, the multilevel function can be accomplished by adjustable applied bias without any external current compliance element. Fig. 4(a) shows the  $I$ - $V$  curves of the one-step set process device, which using different stopping biases of  $-0.5$ ,  $-0.6$ , and  $-0.7$  V during the set process can induce multi-LRS. The LRS decrease can suggest an increasing tendency in the conductive path size. Then a local Joule heating effect induced the thermal dissolution phenomenon prefers to occur neighboring the ITO interface, causing an abrupt reset behavior. Hence, Fig. 4(a) shows that the  $I_{\text{reset}}$  reveals an obviously increasing trend, but is accompanied by an approximate constant trend of  $V_{\text{reset}}$  [15], [16]. Finally, Fig. 4(b) shows the statistical data of multi-LRS while undergoing 100 cycling operations, and indicates that this structure can possess a stable and adjustable self-compliance property.

#### IV. CONCLUSION

Using ITO layer as an electrode dominated the polarity of the bipolar resistance switching in an ITO/Gd:SiO<sub>x</sub>/TiN structure. The interface formation between ITO and Gd:SiO<sub>x</sub>

acted as a series resistor, thereby inducing a self-compliance function for ReRAM. Moreover, a higher current compliance electroforming process resulted in more oxygen ions, which drifted to ITO to form a stronger series resistor, inducing a better self-compliance function for ReRAM and a reduction in operation current.

#### REFERENCES

- [1] H. E. Maes, J. Witters, and G. Groeseneken, "Trends in non-volatile memory devices and technologies," presented at the 17th Eur. Solid State Devices Res. Conf., Bologna, Italy, 1987.
- [2] T. C. Chang, F. Y. Jian, S. C. Chen, and Y. T. Tsai, "Developments in nanocrystal memory," *Mater. Today*, vol. 14, no. 12, pp. 608–615, Dec. 2011.
- [3] C. T. Tsai, T. C. Chang, S. C. Chen, I. Lo, S. W. Tsao, M. C. Hung, J. J. Chang, C. Y. Wu, and C. Y. Huang, "Influence of positive bias stress on N<sub>2</sub>O plasma improved InGaZnO thin film transistor," *Appl. Phys. Lett.*, vol. 96, no. 24, pp. 242105-1–242105-3, 2010.
- [4] T. C. Chen, T. C. Chang, C. T. Tsai, T. Y. Hsieh, S. C. Chen, C. S. Lin, M. C. Hung, C. H. Tu, J. J. Chang, and P. L. Chen, "Behaviors of InGaZnO thin film transistor under illuminated positive gate-bias stress," *Appl. Phys. Lett.*, vol. 97, no. 11, pp. 112104-1–112104-3, 2010.
- [5] H. C. Tseng, T. C. Chang, J. J. Huang, P. C. Yang, Y. T. Chen, F. Y. Jian, S. M. Sze, and M. J. Tsai, "Investigating the improvement of resistive switching trends after post-forming negative bias stress treatment," *Appl. Phys. Lett.*, vol. 99, no. 13, pp. 132104-1–132104-3, 2011.
- [6] J. J. Huang, T. C. Chang, J. B. Yang, S. C. Chen, P. C. Yang, Y. T. Chen, H. C. Tseng, S. M. Sze, A. K. Chu, and M. J. Tsai, "Influence of oxygen concentration on resistance switching characteristics of gallium oxide," *IEEE Electron Device Lett.*, vol. 33, no. 10, pp. 1387–1389, Oct. 2012.
- [7] M. C. Chen, T. C. Chang, C. T. Tsai, S. Y. Huang, S. C. Chen, C. W. Hu, S. M. Sze, and M. J. Tsai, "Influence of electrode material on the resistive memory switching property of indium gallium zinc oxide thin films," *Appl. Phys. Lett.*, vol. 96, no. 26, pp. 262110-1–262110-3, 2010.
- [8] D. Landheer, X. Wu, J. Morais, I. J. R. Baumvol, R. P. Pezzi, L. Miotti, W. N. Lennard, and J. K. Kim, "Thermal stability and diffusion in gadolinium silicate gate dielectric films," *Appl. Phys. Lett.*, vol. 79, no. 16, pp. 2618–2620, 2001.
- [9] Y. E. Syu, T. C. Chang, T. M. Tsai, Y. C. Hung, K. C. Chang, M. J. Tsai, M. J. Kao, and S. M. Sze, "Redox reaction switching mechanism in RRAM device with Pt/CoSiO<sub>x</sub>/TiN structure," *IEEE Electron Device Lett.*, vol. 32, no. 4, pp. 545–547, Apr. 2011.
- [10] Y. E. Syu, T. C. Chang, T. M. Tsai, G. W. Chang, K. C. Chang, Y. H. Tai, M. J. Tsai, Y. L. Wang, S. M. Sze, "Silicon introduced effect on resistive switching characteristics of WO<sub>x</sub> thin films," *Appl. Phys. Lett.*, vol. 100, no. 2, pp. 022904-1–022904-4, 2001.
- [11] K. K. Chiang, J. S. Chen, and J. J. Wu, "Aluminum electrode modulated bipolar resistive switching of Al/fuel-assisted NiO<sub>x</sub>/ITO memory devices modeled with a dual-oxygen-reservoir structure," *ACS Appl. Mater. Inter.*, vol. 4, no. 8, pp. 4237–4245, 2012.
- [12] Z. Wang, W. G. Zhu, A. Y. Du, L. Wu, Z. Fang, X. A. Tran, W. J. Liu, K. L. Zhang, and H.-Y. Yu, "Highly uniform, self-compliance, and forming-free ALD HfO<sub>2</sub>-based RRAM with Ge doping," *IEEE Trans. Electron Devices*, vol. 59, no. 4, pp. 1203–1208, Apr. 2012.
- [13] C. B. Lee, D. S. Lee, A. Benayad, S. R. Lee, M. Chang, M. J. Lee, J. Hur, Y. B. Kim, C. J. Kim, and U.-I. Chung, "Highly uniform switching of tantalum embedded amorphous oxide using self-compliance bipolar resistive switching," *IEEE Electron Device Lett.*, vol. 32, no. 3, pp. 399–401, Mar. 2011.
- [14] S. Yu and H.-S. P. Wong, "A phenomenological model for the reset mechanism of metal oxide RRAM," *IEEE Electron Device Lett.*, vol. 31, no. 12, pp. 1455–1457, Dec. 2010.
- [15] S. Long, C. Cagli, D. Lelmini, M. Liu, and J. Sune, "Analysis and modeling of resistive switching statistics," *J. Appl. Phys.*, vol. 111, no. 7, pp. 074508-1–074508-19, 2012.
- [16] S. Long, C. Cagli, D. Lelmini, M. Liu, and J. Sune, "Reset statistics of NiO-based resistive switching memories," *IEEE Electron Device Lett.*, vol. 32, no. 11, pp. 1570–1572, Nov. 2011.